Mathematical analysis and time-domain simulation of invisibility cloaks with metamaterials

Jichun Li
University of Nevada Las Vegas (UNLV)

Supported by: NSF DMS-1416742.

Collaborators: Y. Huang, W. Yang (Xiangtan Univ), A. Wood (Air Force Institute of Technology)

Invisibility cloak with metamaterials

• Science, vol.312 (June 23, 2006): "Controlling Electromagnetic Fields" (by J.B. Pendry, D. Schurig, D.R. Smith) [Cited 4510 times as Feb.25, 2015, 5118 times as Jan.11, 2016]

• Science, vol.312 (June 23, 2006): "Optical Conformal Mapping" (by Ulf Leonhardt). [Cited 2369 times as Feb.25,2015, 2657 times on $1/11/16$]

• Science, vol.314 (Nov. 10, 2006): "Metamaterial Electromagnetic Cloak at Microwave Frequencies" (by Schurig, Mock, etc.) [Cited 3689 times as Feb.25, 2016, 4163 times on $1/11/16$]

• Greenleaf, Lassas and Uhlmann (2003): For $\nabla \cdot \sigma \nabla u = 0$, question of uniqueness of determination of σ from DN map: $u|_{\partial\Omega} \to \nu \cdot \sigma \nabla u|_{\partial\Omega}$.

• Approx cloaks via anomalous localized resonance: Milton and Nicorovici (May 3, 2006). Further works by Bouchitte, Schweizer (2010), Ammari etc (2013), Kohn, Weinstein etc (2014), ...

• Approximate/near cloaking: for electric impedance tomography (Kohn, Weinstein 2008), for scalar waves governed by Helmholtz equ.(Ammari, H.Y. Liu), for full Maxwell equs (G. Bao, J. Zou),...

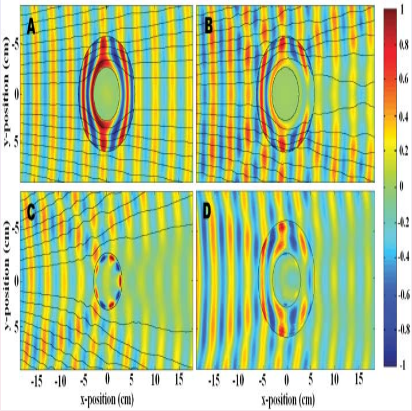

Figure: (A) The simulation of the cloak with the exact material properties, (B) the simulation of the cloak with the reduced material properties, (C) the experimental measurement of the bare conducting cylinder, and (D) the experimental measurement of the cloaked conducting cylinder. Source: D. Schurig et al, Science, V.314, Nov. 2006, 977-980. Invisible to an incident plane wave at 8.5 GHz.

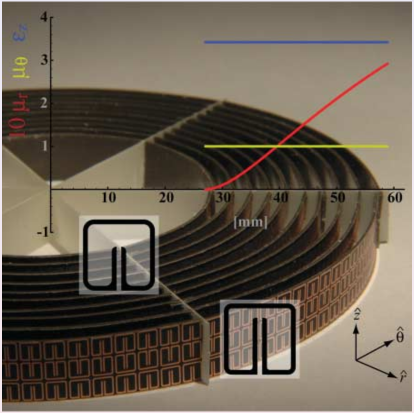

Figure: 2D microwave cloaking structure (background image) with a plot of the material parameters that are implemented. Source: D. Schurig et al, Science, V.314, Nov. 2006, 977-980. Reduced parameters:
$\varepsilon_z = (\frac{b}{b-a})^2, \mu_r = (\frac{r-a}{r})^2, \mu_\theta = 1$. Exact parameters:
$\varepsilon_z = (\frac{b}{b-a})^2 \frac{r-a}{r}, \mu_r = \frac{r-a}{r}, \mu_\theta = \frac{r}{r-a}$

Form invariant property for Maxwell's equations

Theorem

Under a coordinate transformation $x' = x'(x)$, the Maxwell's equations

$$\nabla \times E + j\omega\mu H = 0, \quad \nabla \times H - j\omega\varepsilon E = 0, \tag{1}$$

keep the same form in the transformed coordinate system:

$$\nabla' \times E' + j\omega\mu' H' = 0, \quad \nabla' \times H' - j\omega\varepsilon' E' = 0, \tag{2}$$

where all new variables are given by

$$E'(x') = A^{-T}E(x), \; H'(x') = A^{-T}H(x), \; A = (a_{ij}), \; a_{ij} = \frac{\partial x'_i}{\partial x_j}, \tag{3}$$

and

$$\mu'(x') = A\mu(x)A^T/det(A), \quad \varepsilon'(x') = A\varepsilon(x)A^T/det(A). \tag{4}$$

Proof of form invariant property: Post 1962, Milton 2006

From Maxwell's equations, we have

$$j\omega\mu' H' = j\omega A\mu H/det(A) = -A\nabla \times E/det(A).$$

Hence to prove the first identity of (2), we just need to show that

$$A\nabla \times E = det(A) \cdot \nabla' \times E'. \tag{5}$$

Recall the 3-D Levi-Civita symbol ε_{ijk}, which is 1 if (i,j,k) is an even permutation of $(1,2,3)$, -1 if it is an odd permutation, and 0 if any index is repeated. Hence by using the Einstein notation (i.e., omitting the summation symbols), we have

$$det(A) = \varepsilon_{ijk} \frac{\partial x_1'}{\partial x_i} \frac{\partial x_2'}{\partial x_j} \frac{\partial x_3'}{\partial x_k}, \tag{6}$$

and the ith component of $\nabla \times E$: $(\nabla \times E)_i = \varepsilon_{ijk} \frac{\partial E_k}{\partial x_j}$, from which and $E = A^T E'$, we obtain

Proof of form invariant property: cont'd

$$(A\nabla \times E)_i = \frac{\partial x'_i}{\partial x_m}\varepsilon_{mjk}\frac{\partial E_k}{\partial x_j} = \frac{\partial x'_i}{\partial x_m}\varepsilon_{mjk}\frac{\partial}{\partial x_j}(\frac{\partial x'_l}{\partial x_k}E'_l)$$

$$= \frac{\partial x'_i}{\partial x_m}\varepsilon_{mjk}(\frac{\partial^2 x'_l}{\partial x_j \partial x_k}E'_l + \frac{\partial x'_l}{\partial x_k}\frac{\partial E'_l}{\partial x_j})$$

$$= \frac{\partial x'_i}{\partial x_m}\varepsilon_{mjk}\frac{\partial x'_l}{\partial x_k}\frac{\partial E'_l}{\partial x_j} = \frac{\partial x'_i}{\partial x_m}\varepsilon_{mjk}\frac{\partial x'_l}{\partial x_k}\frac{\partial E'_l}{\partial x'_p}\frac{\partial x'_p}{\partial x_j}. \quad (7)$$

On the other hand, we have

$$det(A)\cdot(\nabla' \times E')_i = det(A)\cdot \varepsilon_{ipl}\frac{\partial E'_l}{\partial x'_p}. \quad (8)$$

Comparing (7) with (8), the proof of (5) boils down to proof of the following $\frac{\partial x'_i}{\partial x_m}\varepsilon_{mjk}\frac{\partial x'_l}{\partial x_k}\frac{\partial x'_p}{\partial x_j} = det(A)\cdot\varepsilon_{ipl}$, which is true by checking different i, p, l. For example, $i = 1, p = 2, l = 3$ is just (6).

Carpet cloak: Li, Huang, Yang, Wood, SIAM J Appl Math (2014)

Following Chen, Pendry, et al [Nature Communications, 2 (2011)], a triangular carpet cloak can be achieved with spatially homogeneous anisotropic dielectric materials.

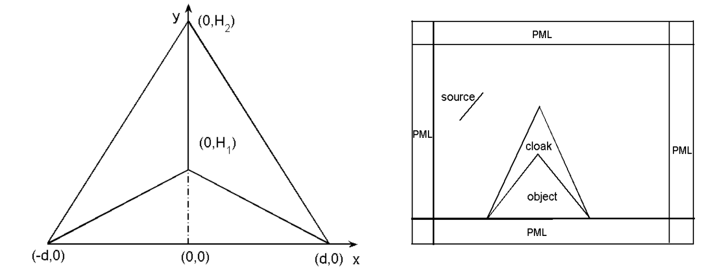

Figure: The physical space of the carpet cloak.

Carpet cloak modeling equations

Using mapping $x' = x, y' = \frac{H_2 - H_1}{H_2} y + \frac{d - xsgn(x)}{d} H_1$ $((x = 0, y = 0)$ maps to $(x' = 0, y' = H_1)$,$(x = d, y = 0)$ maps to $(x' = d, y' = 0)$,), we have

$$A = \begin{bmatrix} \frac{\partial x'}{\partial x} & \frac{\partial x'}{\partial y} \\ \frac{\partial y'}{\partial x} & \frac{\partial y'}{\partial y} \end{bmatrix} = \begin{bmatrix} 1 & 0 \\ -\frac{sgn(x)}{d} H_1 & \frac{H_2 - H_1}{H_2} \end{bmatrix},$$

which leads to $AA^T = \begin{bmatrix} 1 & -\frac{sgn(x)}{d} H_1 \\ -\frac{sgn(x)}{d} H_1 & (\frac{H_2 - H_1}{H_2})^2 + (\frac{H_1}{d})^2. \end{bmatrix}$ The relative permittivity and permeability of the cloak:

$$\varepsilon = \begin{bmatrix} a & b \\ b & c \end{bmatrix} = \begin{bmatrix} \frac{H_2}{H_2 - H_1} & -\frac{H_1 H_2}{(H_2 - H_1)d} \mathrm{sgn}(x) \\ -\frac{H_1 H_2}{(H_2 - H_1)d} \mathrm{sgn}(x) & \frac{H_2 - H_1}{H_2} + \frac{H_2}{H_2 - H_1} (\frac{H_1}{d})^2 \end{bmatrix},$$

$$\mu = \frac{H_2}{H_2 - H_1},$$

where $\mathrm{sgn}(x)$ denotes the standard sign function.

Carpet cloak modeling equations: cont'd

Diagonalizing the symmetric matrix ε as:

$$\varepsilon = P \Sigma P^T, \tag{9}$$

where $\lambda_1 = \frac{a+c-\sqrt{(a-c)^2+4b^2}}{2}$, $\lambda_2 = \frac{a+c+\sqrt{(a-c)^2+4b^2}}{2}$, and matrices Σ and P are

$$\Sigma = \begin{pmatrix} \lambda_1 & 0 \\ 0 & \lambda_2 \end{pmatrix}, \quad P = \begin{pmatrix} p_1 & p_2 \\ p_3 & p_4 \end{pmatrix},$$

and elements $p_i, 1 \leq i \leq 4$, are given as

$$p_1 = \sqrt{\frac{\lambda_2 - a}{\lambda_2 - \lambda_1}}, \quad p_2 = \sqrt{\frac{a - \lambda_1}{\lambda_2 - \lambda_1}} \cdot \mathrm{sgn}(x),$$

$$p_3 = -\sqrt{\frac{\lambda_2 - c}{\lambda_2 - \lambda_1}} \cdot \mathrm{sgn}(x), \quad p_4 = \sqrt{\frac{c - \lambda_1}{\lambda_2 - \lambda_1}}.$$

Carpet cloak modeling equations: cont'd

It is easy to see that $\lambda_2 \geq \frac{a+c+|a-c|}{2} \geq a > 1$, which leads to $\lambda_1 = 1/\lambda_2 < 1$. Mapping λ_1 by the lossless Drude dispersion model:

$$\lambda_1(\omega) = 1 - \frac{\omega_p^2}{\omega^2},$$

where ω_p is plasma frequency, and ω is wave frequency. Substituting $\varepsilon = P\Sigma P^T$ into $D = \varepsilon_0 \varepsilon E$, we obtain

$$\varepsilon_0 E = P\Sigma^{-1} P^T D,$$

which equals to

$$\varepsilon_0 E_x = \lambda_1^{-1}(p_1^2 D_x + p_1 p_3 D_y) + \lambda_2^{-1}(p_2^2 D_x + p_2 p_4 D_y),$$
$$\varepsilon_0 E_y = \lambda_1^{-1}(p_1 p_3 D_x + p_3^2 D_y) + \lambda_2^{-1}(p_2 p_4 D_x + p_4^2 D_y).$$

We can rewrite these equations as:

$$\varepsilon_0 \lambda_2(-\omega^2 + \omega_p^2) E_x = (-\omega^2)\lambda_2(p_1^2 D_x + p_1 p_3 D_y) + (-\omega^2 + \omega_p^2)(p_2^2 D_x + p_2 p_4 D_y),$$
$$\varepsilon_0 \lambda_2(-\omega^2 + \omega_p^2) E_y = (-\omega^2)\lambda_2(p_1 p_3 D_x + p_3^2 D_y) + (-\omega^2 + \omega_p^2)(p_2 p_4 D_x + p_4^2 D_y).$$

Carpet cloak modeling equations: cont'd

The above equations can be written in time-domain (assuming $e^{i\omega t}$ time dependence):

$$\varepsilon_0\lambda_2(\partial_{t^2}+\omega_p^2)E_x = \lambda_2\partial_{t^2}(p_1^2 D_x + p_1 p_3 D_y) + (\partial_{t^2}+\omega_p^2)(p_2^2 D_x + p_2 p_4 D_y),$$
$$\varepsilon_0\lambda_2(\partial_{t^2}+\omega_p^2)E_y = \lambda_2\partial_{t^2}(p_1 p_3 D_x + p_3^2 D_y) + (\partial_{t^2}+\omega_p^2)(p_2 p_4 D_x + p_4^2 D_y).$$

which equal to

$$\varepsilon_0\lambda_2\left(E_{t^2}+\omega_p^2 E\right) = M_A D_{t^2} + M_B D, \tag{10}$$

where matrices M_A and M_B are

$$M_A = \begin{pmatrix} p_1^2\lambda_2 + p_2^2 & p_2 p_4 + p_1 p_3\lambda_2 \\ p_2 p_4 + p_1 p_3 \lambda_2 & p_3^2\lambda_2 + p_4^2 \end{pmatrix}, \quad M_B = \begin{pmatrix} p_2^2 & p_2 p_4 \\ p_2 p_4 & p_4^2 \end{pmatrix}\omega_p^2.$$

Carpet cloak modeling equations: cont'd

The governing equations for the carpet cloak:

$$D_t = \nabla \times H, \tag{11}$$

$$\varepsilon_0 \lambda_2 \left(E_{t^2} + \omega_p^2 E \right) = M_A D_{t^2} + M_B D, \tag{12}$$

$$\mu_0 \mu H_t = -\nabla \times E, \tag{13}$$

supplemented with initial conditions

$$D(x,0) = D_0(x), \quad E(x,0) = E_0(x), \quad H(x,0) = H_0(x), \quad \forall\, x \in \Omega, \tag{14}$$

and the perfect conducting boundary condition (PEC):

$$n \times E = \mathbf{0} \quad \text{on } \partial\Omega. \tag{15}$$

Here H denotes the magnetic field, and 2D vector and scalar curl operators:

$$\nabla \times H = (\frac{\partial H}{\partial y}, -\frac{\partial H}{\partial x})', \quad \nabla \times E = \frac{\partial E_y}{\partial x} - \frac{\partial E_x}{\partial y}, \;\; \forall E = (E_x, E_y)'.$$

Carpet cloak equations: existence

Lemma

The matrix M_B is symmetric and non-negative definite, and the matrix M_A is symmetric positive definite.

Proof. For any vector $(u,v)'$, we have

$$(u,v)M_B\begin{pmatrix} u \\ v \end{pmatrix} = \omega_p^2(p_2u + p_4v)^2 \geq 0,$$

and

$$(u,v)M_A\begin{pmatrix} u \\ v \end{pmatrix} = \lambda_2(p_1u + p_3v)^2 + (p_2u + p_4v)^2 > 0.$$

Carpet cloak equations: existence

Theorem

For any $t \in [0, T]$, there exists a unique solution $(E(\cdot, t), H(\cdot, t)) \in (H_0(curl; \Omega)) \times H(curl; \Omega)$ of (11)-(15).

Proof. Denote Laplace transform by $\hat{u}(s) = \mathscr{L}(u) = \int_0^\infty e^{-st} u(t) dt$. Taking the Laplace transforms of (11)–(13), we obtain

$$s\hat{D} - D_0 = \nabla \times \hat{H}, \tag{16}$$

$$\begin{aligned} &\varepsilon_0 \lambda_2 \left(s^2 \hat{E} - sE_0 - \partial_t E(0) + \omega_p^2 \hat{E} \right) \\ &\quad = M_A \left(s^2 \hat{D} - sD_0 - \partial_t D(0) \right) + M_B \hat{D}, \end{aligned} \tag{17}$$

$$\mu_0 \mu (s\hat{H} - H_0) = -\nabla \times \hat{E}. \tag{18}$$

Eliminating $\hat{D}, \hat{H}$, we obtain

$$\begin{aligned} & \varepsilon_0 \mu_0 \mu \lambda_2 (s^4 + s^2 \omega_p^2) \hat{E} \\ = \ & (s^2 M_A + M_B)(\mu_0 \mu \nabla \times \hat{H}_0 - \nabla \times \nabla \times \hat{E}) + \mu_0 \mu s f_0(s), \end{aligned}$$

Carpet cloak equations: existence

which has a weak formulation as follows: Find $\hat{E} \in H_0(\text{curl};\Omega)$ such that

$$\epsilon_0\mu_0\mu\lambda_2(s^4+s^2\omega_p^2)(\hat{E},u)+(s^2M_A+M_B)(\nabla\times\hat{E},\nabla\times u)=(F_0(s),u) \tag{19}$$

holds true for any $u \in H_0(\text{curl};\Omega)$. Here
$F_0(s)=\mu_0\mu(s^2M_A+M_B)\nabla\times\hat{H}_0+\mu_0\mu s f_0(s)$, and

$$f_0(s)=\epsilon_0\lambda_2(s^2E_0+s\partial_t E(0))+(s^2M_A+M_B)D_0-sM_A(sD_0-\partial_t D(0)).$$

The existence of a unique solution $\hat{E} \in H_0(\text{curl};\Omega)$ of (19) is guaranteed by the Lax-Milgram lemma.

Carpet cloak equations: stability

Theorem

For the solution (D, E) *of (11)–(13) and any* $t \in [0, T]$*, the following stability holds true:*

$$\begin{aligned} & \left(||\sqrt{M_A}D_t||^2 + ||\sqrt{M_B}D||^2 + ||E_{t^2}||^2 + ||E_t||^2 + ||E||^2 + ||\sqrt{M_A}\nabla \times E_t||^2\right)(t) \\ \leq \quad & C\left(||\sqrt{M_A}D_t||^2 + ||\sqrt{M_B}D||^2 + ||E_{t^2}||^2 + ||E_t||^2 + ||E||^2 + ||\sqrt{M_A}\nabla \times E_t||^2\right)(0), \end{aligned}$$

where the constant $C > 0$ *depends on the physical parameters* $\varepsilon_0, \mu_0, d, H_1, H_2$ *and* ω_p.

The Finite element time-domain (FETD) scheme

Denote difference and average operators:

$$\delta_\tau u^n = \frac{u^n - u^{n-1}}{\tau}, \quad \delta_\tau^2 u^n = \frac{u^n - 2u^{n-1} + u^{n-2}}{\tau^2},$$
$$\hat{u}^{n+\frac{1}{2}} = \frac{u^{n+\frac{1}{2}} + u^{n-\frac{1}{2}}}{2}, \quad \check{u}^{n+\frac{1}{2}} = \frac{u^{n+\frac{1}{2}} + 2u^{n-\frac{1}{2}} + u^{n-\frac{3}{2}}}{4} = \frac{\hat{u}^{n+\frac{1}{2}} + \hat{u}^{n-\frac{1}{2}}}{2}.$$

Construct a leap-frog scheme for the model equations (11)-(13): Given approximations $H_h^0, D_h^{-\frac{1}{2}}, D_h^{-\frac{3}{2}}, E_h^{-\frac{1}{2}}, E_h^{-\frac{3}{2}}$, find $D_h^{n+\frac{1}{2}}, E_h^{n+\frac{1}{2}} \in V_h^0$, $H_h^{n+1} \in U_h$ such that

$$\left(\delta_\tau D_h^{n+\frac{1}{2}}, \phi_h\right) = (H_h^n, \nabla \times \phi_h), \tag{20}$$
$$\epsilon_0\lambda_2 \left(\delta_\tau^2 E_h^{n+\frac{1}{2}}, \varphi_h\right) + \epsilon_0\lambda_2\omega_p^2 \left(\check{E}_h^{n+\frac{1}{2}}, \varphi_h\right) = \left(M_A \delta_\tau^2 D_h^{n+\frac{1}{2}}, \varphi_h\right) + \left(M_B \check{D}_h^{n+\frac{1}{2}}, \varphi_h\right), \tag{21}$$
$$\mu_0\mu \left(\delta_\tau H_h^{n+1}, \psi_h\right) = -(\nabla \times E_h^{n+\frac{1}{2}}, \psi_h), \tag{22}$$

hold true for any ϕ_h, $\varphi_h \in V_h^0$, $\psi_h \in U_h$.

The FETD scheme: cont'd

For rectangular elements $K \in T^h$,

$$U_h = \{\psi_h \in L^2(\Omega): \ \ \psi_h|_K \in Q_{0,0}, \ \forall\ K \in T^h\},$$
$$\boldsymbol{V}_h = \{\phi_h \in H(curl;\Omega): \ \ \phi_h|_K \in Q_{0,1} \times Q_{1,0}, \ \forall\ K \in T^h\},$$

where $Q_{i,j}$ denotes the space of polynomials whose degrees are less than or equal to i and j in variables x and y, respectively.
While for triangular elements, we choose

$$U_h = \{\psi_h \in L^2(\Omega): \ \ \psi_h|_K \text{ is a piecewise constant}, \ \forall\ K \in T^h\},$$
$$\boldsymbol{V}_h = \{\phi_h \in H(curl;\Omega): \ \ \phi_h|_K = \text{span}\{L_i\nabla L_j - L_j\nabla L_i\}, \ i,j = 1,2,3, \forall\ K$$

where L_i denotes the standard linear basis function at vertex i of element K. The space

$$\boldsymbol{V}_h^0 = \{\phi_h \in \boldsymbol{V}_h, \ \ n \times \phi_h = \boldsymbol{0} \ \text{ on } \partial\Omega\}$$

is introduced to impose the perfect conducting boundary condition $n \times E = \boldsymbol{0}$.

The FETD scheme: discrete stability

Theorem

Denote the solution $(D_h^{n+\frac{1}{2}}, E_h^{n+\frac{1}{2}})$ *of (20)–(22), and the discrete energy*

$$ENG_n = \frac{\varepsilon_0\mu_0\mu\lambda_2(2+\omega_p^2)}{4}||\delta_\tau E_h^{n+\frac{1}{2}}||^2 + \frac{\varepsilon_0\mu_0\mu\lambda_2\omega_p^2}{2}||\hat{E}_h^{n+\frac{1}{2}}||^2 + \frac{1}{2}||\sqrt{M_A}\nabla\times E_h^{n+\frac{1}{2}}||^2$$
$$+\frac{1}{2}||\sqrt{M_A}\delta_\tau D_h^{n+\frac{1}{2}}||^2 + \frac{1}{2}||\sqrt{M_B}\hat{D}_h^{n+\frac{1}{2}}||^2 + \frac{\varepsilon_0\mu_0\mu\lambda_2}{2}||\delta_\tau^2 E_h^{n+\frac{1}{2}}||^2 + \frac{1}{2}||\sqrt{M_A}\nabla\times\delta_\tau E_h^{n+\frac{1}{2}}||^2.$$

Then for any $m \geq 1$ *and a small constant* $C_{cfl} > 0$*, under the constraint*

$$\tau \leq C_{cfl}h^2, \tag{23}$$

we have

$$ENG_m \leq C\left(ENG_0 + ||\sqrt{M_A}\nabla\times E_h^{-\frac{1}{2}}||^2 + ||\delta_\tau E_h^{-\frac{1}{2}}||^2 + ||\sqrt{M_B}\delta_\tau D_h^{-\frac{1}{2}}||^2\right).$$

Numerical results: PML

To simulate the cloak phenomenon, we surround the physical domain by a perfectly matched layer (PML), see Fig.3 (Right). In this paper, we use the classical 2D Berenger PML, whose governing equations can be written as

$$\varepsilon_0 \frac{\partial \boldsymbol{E}}{\partial t} + \begin{pmatrix} \sigma_y & 0 \\ 0 & \sigma_x \end{pmatrix} \boldsymbol{E} = \nabla \times H_z, \tag{24}$$

$$\mu_0 \frac{\partial H_{zx}}{\partial t} + \sigma_{mx} H_{zx} = -\frac{\partial E_y}{\partial x}, \tag{25}$$

$$\mu_0 \frac{\partial H_{zy}}{\partial t} + \sigma_{my} H_{zy} = \frac{\partial E_x}{\partial y}, \tag{26}$$

where $H_z = H_{zx} + H_{zy}$ denotes the magnetic field, the parameters σ_i and $\sigma_{m,i}, i = x, y$, are the electric and magnetic conductivities in the x- and y- directions, respectively. In our simulation, we use a PML with 12 rectangular cells in thickness around the physical domain.

Numerical examples: Ex 1

In our simulation, we choose $H_1 = 0.05m, H_2 = 0.2m, d = 0.2m$, and the physical domain $\Omega = [-0.3, 0.3]\ m \times [0, 0.3]\ m$, which is partitioned by a uniform triangular mesh with a mesh size $h = 0.00625$. The PML region surrounding Ω is partitioned by a uniform rectangular mesh. Our final mesh yields 53330 total edges, 26960 total triangular elements, and 6258 total rectangular elements. In the test, we choose the time step size $\tau = 2 * 10^{-13}$ s, and the total number of time steps 15000, i.e., the final simulation time $T = 3.0$ nanosecond (ns).
Example 1. The incident wave is generated by a plane wave source $H_z = 0.1\sin(\omega t)$ imposed at line $x = -0.3$, where $\omega = 2\pi f$ with frequency $f = 3.0$ GHz. The numerical magnetic fields H_z at different time steps are shown in Fig.4. Both figures show clearly that the plane wave pattern is recovered very well after passing through the cloaking region, which makes any objects hiden inside the cloaked region invisible to observers at the far end.

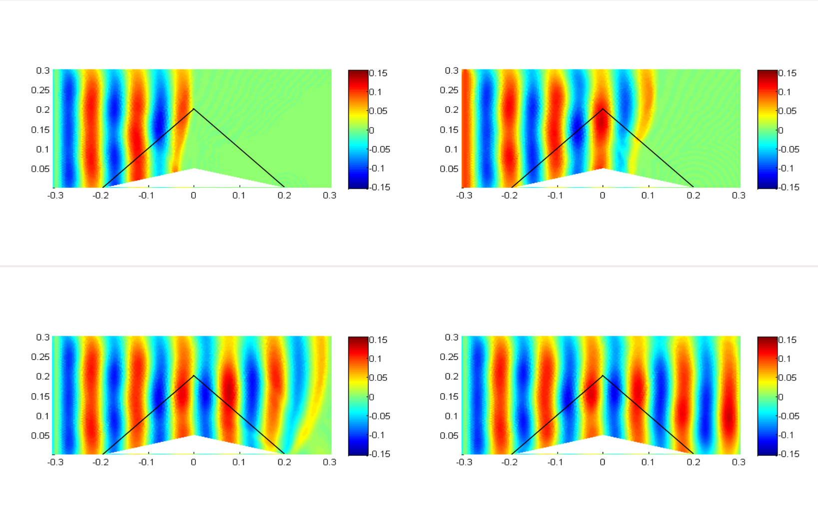

Figure: Ex1. The H_z fields at 5000, 7000, 10000, 15000 time steps.

Numerical examples: Ex 2

Example 2. The incident wave is generated by a Gaussian wave

$$H_z(x,y,t) = 0.1e^{-(y-0.15)^2/(60L)^2}\sin(\omega t)$$

imposed along a slanted line $y = x + 0.45$, where $L = 0.004\sqrt{2}$, and $\omega = 2\pi f$ with frequency $f = 6.0$ GHz. The numerical magnetic fields H_z at different time steps are presented in Fig.5. To appreciate the cloak phenomenon, in Fig.6 we present the magnetic fields H_z obtained without the cloaking material. It is clear that the cloak phenomenon disappears if the cloaking material is removed.

Numerical examples: Ex 2

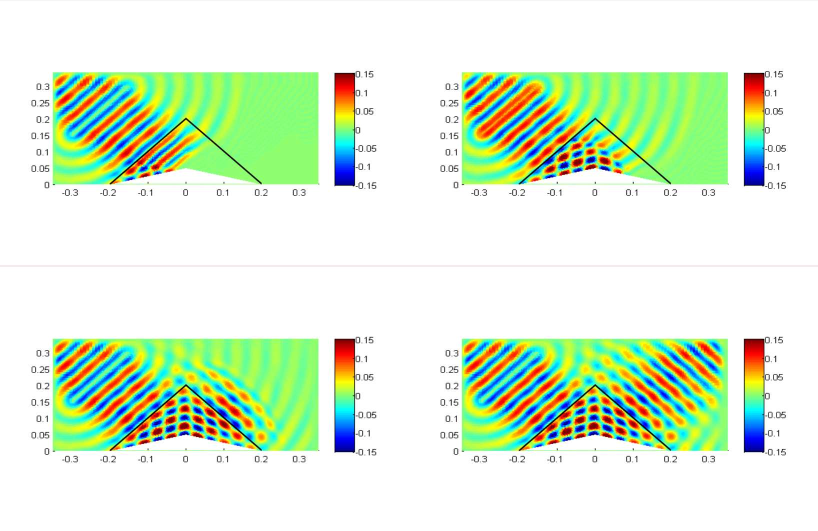

Figure: Ex2. The H_z fields at 5000, 7000, 10000, 15000 time steps.

Numerical examples: Ex 2

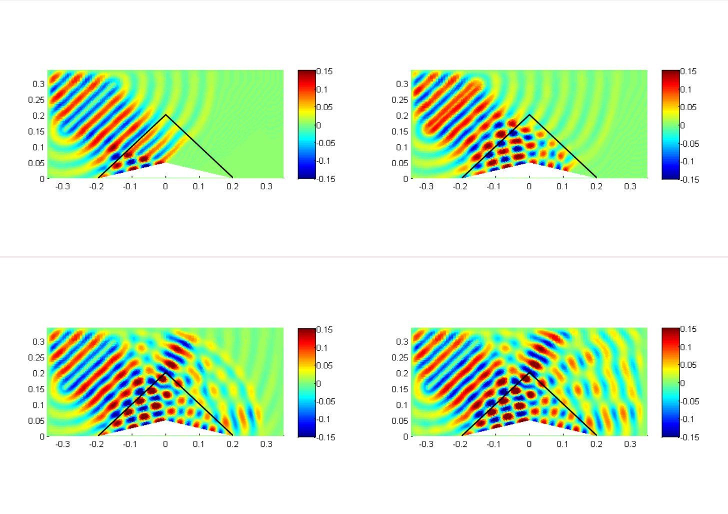

Figure: Ex2. The H_z fields at 5000, 7000, 10000, 15000 time steps obtained with the cloaking material removed.

Numerical examples: Ex 3

Example 3. Since the ideal cloak requires that the permittivity and permeability be anisotropic, which is quite difficult to be constructed. The following reduced cloak material is suggested by Chen, Pendry et al (2011):

$$\mu = 1, \;\; \varepsilon = \frac{H_2}{H_2 - H_1} \begin{bmatrix} \frac{H_2}{H_2-H_1} & -\frac{H_1 H_2}{(H_2-H_1)d}\mathrm{sgn}(x) \\ -\frac{H_1 H_2}{(H_2-H_1)d}\mathrm{sgn}(x) & \frac{H_2-H_1}{H_2} + \frac{H_2}{H_2-H_1}(\frac{H_1}{d})^2 \end{bmatrix},$$

and the reduced cloak materials can be realized by natural anisotropic materials. We solve Example 2 again by using this simplified permittivity and permeability. The calculated magnetic fields H_z at different time steps are presented in Fig.7, which shows that the cloak phenomenon is almost the same as Fig.5 for the ideal permittivity and permeability.

Numerical examples: Ex 3

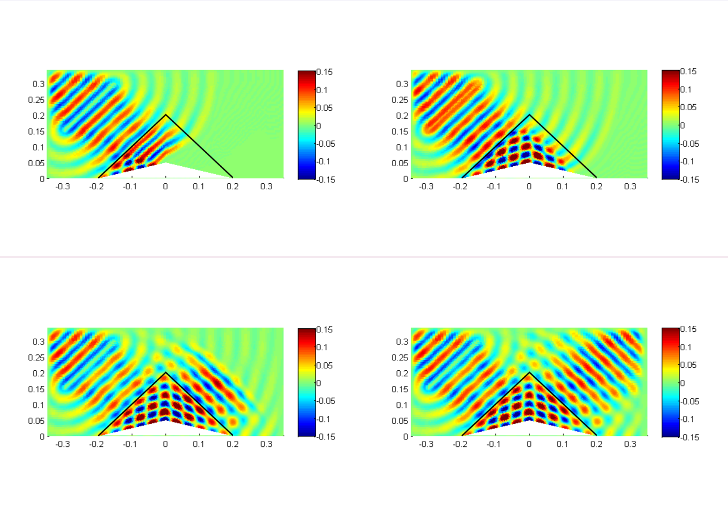

Figure: Ex3. The H_z fields at 5000, 7000, 10000, 15000 time steps obtained with the simplified cloak material.

Cyclindrical cloak in time domain

Cylindrical cloak: Pendry et al (Science 2006):

$$\varepsilon_r = \mu_r = \frac{r - R_1}{r}, \quad \varepsilon_\phi = \mu_\phi = \frac{r}{r - R_1},$$
$$\varepsilon_z = \mu_z = \left(\frac{R_2}{R_2 - R_1}\right)^2 \frac{r - R_1}{r},$$

R_1 and R_2: inner and outer radius of the cloak.
Transforming the polar coordinate system to the Cartesian coordinate system, and using the Drude model for the permittivity:

$$\varepsilon_r(\omega) = 1 - \frac{\omega_p^2}{\omega^2 - j\omega\gamma},$$

we obtain

$$\begin{aligned} & \varepsilon_0 \varepsilon_\phi \left(\frac{\partial^2}{\partial t^2} + \gamma \frac{\partial}{\partial t} + w_p^2 \right) \boldsymbol{E} \\ = \quad & \left(\frac{\partial^2}{\partial t^2} + \gamma \frac{\partial}{\partial t} + w_p^2 \right) M_A \boldsymbol{D} + \varepsilon_\phi \left(\frac{\partial^2}{\partial t^2} + \gamma \frac{\partial}{\partial t} \right) M_B \boldsymbol{D}, \end{aligned}$$

Cyclindrical cloak: cont'd

where we denote $D = (D_x, D_y)'$ and

$$M_A = \begin{bmatrix} \sin^2\phi & -\sin\phi\cos\phi \\ -\sin\phi\cos\phi & \cos^2\phi \end{bmatrix}, \quad M_B = \begin{bmatrix} \cos^2\phi & \sin\phi\cos\phi \\ \sin\phi\cos\phi & \sin^2\phi \end{bmatrix}.$$

Permeability using the Drude model:

$$\mu_z(\omega) = A\left(1 - \frac{\omega_{pm}^2}{\omega^2 - j\omega\gamma_m}\right), \quad A = \frac{R_2}{R_2 - R_1},$$

$\omega_{pm} > 0$ and $\gamma_m \geq 0$: magnetic plasma and collision frequencies.

$$\left(\frac{\partial^2}{\partial t^2} + \gamma_m \frac{\partial}{\partial t}\right) B_z = \mu_0 A \left(\frac{\partial^2}{\partial t^2} + \gamma_m \frac{\partial}{\partial t} + \omega_{pm}^2\right) H_z.$$

Analysis of the model: Li, Huang, Yang (Math Comp, 2015)

Assume that $\gamma = \gamma_m$.

$$\begin{aligned} & \mu_0 A \varepsilon_0 \varepsilon_\phi (E_{t^3} + \gamma E_{t^2} + \omega_p^2 E_t) \\ = \ & \mu_0 A (M_A + \varepsilon_\phi M_B) \nabla \times (H_{t^2} + \gamma H_t) + \mu_0 A \omega_p^2 M_A \nabla \times H. \end{aligned} \tag{27}$$

To simplify the notation, we denote $H = H_z$, $M = M_A + \varepsilon_\phi M_B$.
Also we have

$$\mu_0 A (H_{t^2} + \gamma H_t + \omega_{pm}^2 H) = -\nabla \times E_t - \gamma \nabla \times E. \tag{28}$$

Taking curl of (28) and substituting into (27), we have

$$\begin{aligned} & \mu_0 \varepsilon_0 A \varepsilon_\phi (E_{t^3} + \gamma E_{t^2} + \omega_p^2 E_t) + M \nabla \times \nabla \times E_t + \gamma M \nabla \times \nabla \times E \\ = \ & -\mu_0 A M \nabla \times (\omega_{pm}^2 H) + \mu_0 A \omega_p^2 M_A \nabla \times H. \end{aligned} \tag{29}$$

Analysis of the model: cont'd

Lemma

Matrix M_A is symmetric and non-negative definite, and M is SPD.

Lemma

For matrix $M_C = (M_A + \epsilon_\phi M_B)^{-1}$, $M_C \cdot M_A = M_A$ holds true.

Weak formulation: For any $\phi \in H_0(\text{curl};\Omega), \psi \in L^2(\Omega)$,

$$
\begin{aligned}
(i) \qquad & \epsilon_0\mu_0 A[(\epsilon_\phi M_C E_{t^3},\phi) + \gamma(\epsilon_\phi M_C E_{t^2},\phi) + (\omega_p^2\epsilon_\phi M_C E_t,\phi)] \\
& +(\nabla\times E_t,\nabla\times\phi) + \gamma(\nabla\times E,\nabla\times\phi) \\
= \quad & -\mu_0 A(\omega_{pm}^2 H,\nabla\times\phi) + \mu_0 A(\omega_p^2 M_C M_A \nabla\times H,\phi), \qquad (30) \\
(ii) \qquad & \mu_0 A\left[(H_{t^2},\psi) + \gamma(H_t,\psi) + (\omega_{pm}^2 H,\psi)\right] \\
= \quad & -(\nabla\times E_t + \gamma\nabla\times E,\psi). \qquad (31)
\end{aligned}
$$

Analysis of the model: cont'd

Theorem

For the solution of (30)-(31), the following stability holds true:

$$\begin{aligned}
&\varepsilon_0\mu_0 A[(\varepsilon_\phi M_c E_{t^2}, E_{t^2})(t) + (\omega_p^2 \varepsilon_\phi M_c E_t, E_t)(t)] + (\nabla\times E_t, \nabla\times E_t)(t) \\
&+(\nabla\times E, \nabla\times E)(t) + A(\omega_p^2\varepsilon_\phi M_c E, E)(t) \\
&+\mu_0 A(||H_t||_0^2 + ||\omega_{pm} H||_0^2)(t) \le CF(0), \qquad (32)
\end{aligned}$$

where $F(0)$ depends on initial conditions $\nabla\times E(0), \nabla\times E_t(0), E(0)$, $E_t(0), E_{t^2}(0), H(0), \nabla\times H(0), H_t(0)$ and $D(0)$.

Theorem

For any $t\in[0,T]$, there exists a unique solution $(E(\cdot,t), H(\cdot,t)) \in H_0(curl;\Omega)\times H(curl;\Omega)$ of (30)-(31).

2D PML

2D Berenger's perfectly matched layer (PML):

$$
\begin{aligned}
\varepsilon_0 \frac{\partial E_x}{\partial t} + \sigma_y E_x &= \frac{\partial \left(H_{zx} + H_{zy}\right)}{\partial y}, \\
\varepsilon_0 \frac{\partial E_y}{\partial t} + \sigma_x E_y &= -\frac{\partial \left(H_{zx} + H_{zy}\right)}{\partial x}, \\
\mu_0 \frac{\partial H_{zx}}{\partial t} + \sigma_{mx} H_{zx} &= -\frac{\partial E_y}{\partial x}, \\
\mu_0 \frac{\partial H_{zy}}{\partial t} + \sigma_{my} H_{zy} &= \frac{\partial E_x}{\partial y},
\end{aligned}
$$

$\sigma_i, \sigma_{mi}, i = x, y$: homogeneous electric and magnetic conductivities in the x and y directions.

Mixed FE spaces

Rectangular edge element:

$$\boldsymbol{U}_h = \{\psi_h \in L^2(\Omega): \quad \psi_h|_K \in Q_{0,0}, \ \forall\, K \in T^h\}, \tag{33}$$

$$\boldsymbol{V}_h = \{\phi_h \in H(curl;\Omega): \quad \phi_h|_K \in Q_{0,1} \times Q_{1,0}, \ \forall\, K \in T^h\}, \tag{34}$$

Triangular edge element:

$$\boldsymbol{U}_h = \{\psi_h \in L^2(\Omega): \quad \psi_h|_K \text{ is a piecewise constant}, \ \forall\, K \in T^h\},$$
$$\boldsymbol{V}_h = \{\phi_h \in H(curl;\Omega): \quad \phi_h|_K = \text{span}\{\lambda_i \nabla \lambda_j - \lambda_j \nabla \lambda_i\}, \ i,j = 1,2,3, \forall\, K$$

$$\boldsymbol{V}_h^0 = \{\phi_h \in \boldsymbol{V}_h, \ \ n \times \phi_h = \boldsymbol{0} \ \text{ on } \partial\Omega\}.$$

$$\delta_\tau \boldsymbol{u}^n = \frac{\boldsymbol{u}^n - \boldsymbol{u}^{n-1}}{\tau}, \ \ \delta_\tau^2 \boldsymbol{u}^n = \frac{\boldsymbol{u}^n - 2\boldsymbol{u}^{n-1} + \boldsymbol{u}^{n-2}}{\tau^2},$$
$$\delta_{2\tau} \boldsymbol{u}^n = \frac{\boldsymbol{u}^n - \boldsymbol{u}^{n-2}}{2\tau}, \ \ \overline{\boldsymbol{u}}^{n-1} = \frac{\boldsymbol{u}^n + 2\boldsymbol{u}^{n-1} + \boldsymbol{u}^{n-2}}{4}, \ \ \widehat{\boldsymbol{u}}^n = \frac{\boldsymbol{u}^n + \boldsymbol{u}^{n-1}}{2}.$$

The TD-FEM for cloaking simulation

In the cloak region: for $n = 1, 2, \ldots..$, find $D_h^{n+\frac{1}{2}},\ E_h^{n+\frac{1}{2}} \in V_h^0,\ H_h^n \in U_h$ such that

$$\left(\delta_\tau D_h^{n+\frac{1}{2}}, \phi_h\right) = (H_h^n, \nabla \times \phi_h), \tag{37}$$

$$\begin{aligned}
&\varepsilon_0\left(\varepsilon_\phi \delta_\tau^2 E_h^{n+\frac{1}{2}}, \varphi_h\right) + \varepsilon_0\gamma\left(\varepsilon_\phi \check{E}_h^{n+\frac{1}{2}}, \varphi_h\right) + \varepsilon_0\left(\omega_p^2 \varepsilon_\phi \hat{E}_h^n, \varphi_h\right) \\
&= \left(M\delta_\tau^2 D_h^{n+\frac{1}{2}}, \varphi_h\right) + \gamma\left(M\check{D}_h^{n+\frac{1}{2}}, \varphi_h\right) + \left(\omega_p^2 M_A \hat{D}_h^n, \varphi_h\right),
\end{aligned} \tag{38}$$

$$\begin{aligned}
&\mu_0 A\left((\delta_\tau^2 H_h^{n+1}, \psi_h) + \gamma(\check{H}_h^{n+1}, \psi_h) + (\omega_p^2 \hat{H}_h^{n+\frac{1}{2}}, \psi_h)\right) \\
&= -(\nabla \times \check{E}_h^{n+\frac{1}{2}} + \gamma \nabla \times \hat{E}_h^n, \psi_h)
\end{aligned} \tag{39}$$

hold true for any $\phi_h,\ \varphi_h \in V_h^0,\ \psi_h \in U_h$.

Numerical results: Li, Huang, Yang, Math Comp (2015)

Use $R_1 = 0.1m, R_2 = 0.2m$, $\gamma = \gamma_m = 0$ in our Drude model.

A plane wave source: specified by $H_z = 0.1\sin(\omega t)$, where $\omega = 2\pi f$ with operating frequency $f = 2.0$ GHz.
A point source wave (same H_z) at a point (0:078; 0:4).

Simulation with 65536 triangles, 28672 rectangles, and time step $\tau = 0.2$ps.

Numerical results

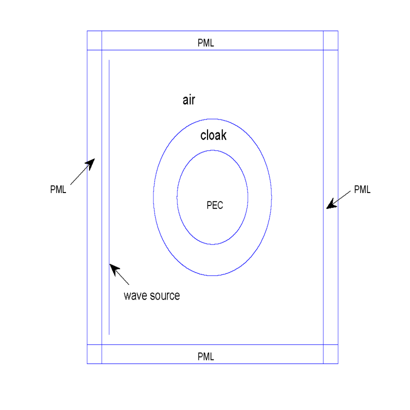

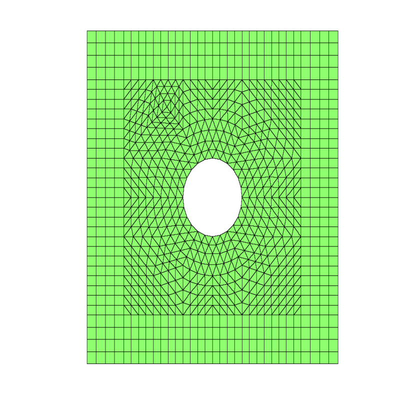

(a) (b)

Figure: *(a): The cloak modeling setup; (b): A coarse mesh.*

Numerical results: plane wave source

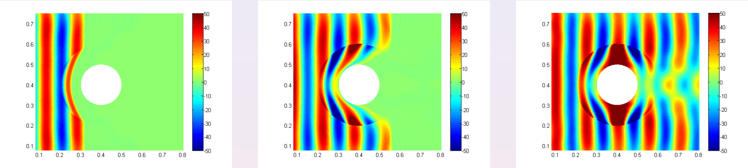

(a) (b) (c)

Figure: E_y at (a) $t = 0.8ns$ ($4000 steps$); (b) $t = 1.6\ ns$; (c) $t = 3.2\ ns$.

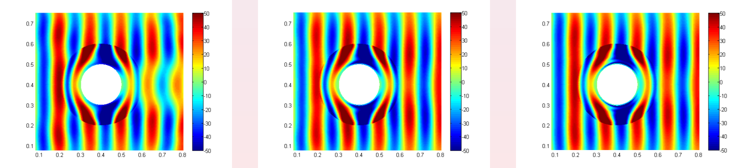

(a) (b) (c)

Figure: E_y at (a) $t = 4.0\ ns$; (b) $t = 6.0\ ns$; (c) $t = 8.0ns$ ($40,000 steps$).

Numerical results: point wave source

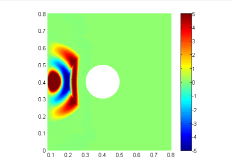

(a)

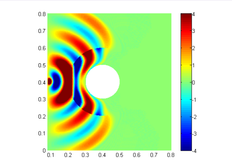

(b)

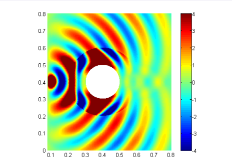

(c)

Figure: E_y at (a) $t = 0.8ns$ ($4000 steps$); (b) $t = 1.6\ ns$; (c) $t = 3.2\ ns$.

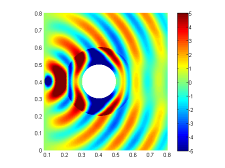

(a)

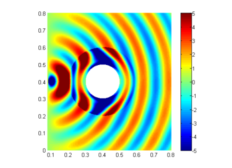

(b)

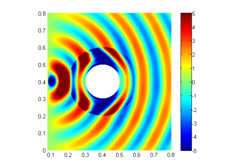

(c)

Figure: E_y at (a) $t = 4.0\ ns$; (b) $t = 6.0\ ns$; (c) $t = 8.0ns$ ($40,000 steps$).

Summary on modeling of metamaterials

J. Li and Y. Huang, Time-Domain Finite Element Methods for Maxwell's Equations in Metamaterials, Springer Series in Computational Mathematics, vol.43, Springer, Jan. 2013, 302pp.

- well-posedness and regularity;
- mass-lumping;
- dispersion and dissipation analysis;
- multiscale technique;
- nonconforming elements;
- fast solvers: DDM, preconditioner,
- a posteriori error estimator; superconvergence;
- hp-adaptivity (including adaptive DG);
- frequency-domain analysis;
- potential applications: solar cell design, black hole, particle detection,....

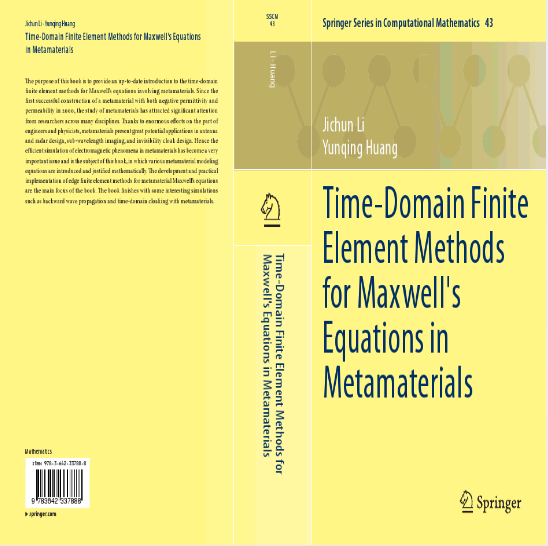

Thanks for your attention!